Aquatic Mammals 2022, *48*(1), 68-74, DOI 10.1578/AM.48.1.2022.68

Ganglion Cell Topography and Retinal Resolution in an Irrawaddy Dolphin (*Orcaella brevirostris*)

Alla M. Mass and Alexander Ya. Supin

Institute of Ecology and Evolution, Russian Academy of Sciences, 33 Leninsky Prospect, 119071 Moscow, Russia
E-mail: alla-mass@mail.ru

Abstract

The topographic distribution of retinal ganglion cells was investigated in a retinal wholemount of an Irrawaddy dolphin (*Orcaella brevirostris*). Two zones of increased concentration of ganglion cells were observed—one in the temporal segment and the other in the nasal segment of the retina. The maximal cell concentration was 250 cell/mm^2 in the temporal area and 194 cell/mm^2 in the nasal area. Based on the posterior nodal distance of 11 mm, the resolution was evaluated as 19.8 arc min in the temporal retinal area (the frontal visual field) and 22.4 arc min in the nasal retinal area (the temporal visual field). Among retinal ganglion cells, a group of giant cells that ranged from 42 to 52 µm in diameter were observed; these cells represented 8% of the total population. The obtained data allowed us to suggest that the presence of two areas of concentrated ganglion cells is characteristic of many delphinids inhabiting both clear oceanic waters or turbid river waters, whereas low ganglion cell density is associated with optic properties of the media.

Key Words: retinal wholemount, retinal topography, retinal resolution, Irrawaddy dolphin, *Orcaella brevirostris*

Introduction

Cetaceans feature unique retinal organization. The majority of terrestrial mammals have one zone of high resolution in their retina: the fovea, area centralis, or visual streak (Hughes, 1977; Collin, 1999). Several large-bodied terrestrial mammals (the elephant, hippopotamus, and rhinoceros) have more than one area of increased retinal resolution (Pettigrew & Manger, 2008; Pettigrew et al., 2010; Coimbra & Manger, 2017; Coimbra et al., 2017); however, the single-area retinal organization is mostly typical. The majority of cetaceans have two high-resolution zones in the temporal and nasal sectors of the retina. This type of retinal organization is characteristic of many marine cetaceans. This organization is described in a number of odontocetes, specifically, the common dolphin (*Delphinus delphis*; Dral, 1983), harbor porpoise (*Phocoena phocoena*; Mass & Supin, 1986), bottlenose dolphin (*Tursiops truncatus*; Mass & Supin, 1995), Dall's porpoise (*Phocoenoides dalli*; Murayama et al., 1995), beluga (*Dephinapterus leucas*; Murayama & Somiya, 1998; Mass & Supin, 2002), Pacific white-sided dolphin (*Lagenorhynchus obliquidens*; Murayama & Somiya, 1998), and killer whale (*Orcinus orca*; Mass et al., 2013), as well as in several mysticetes, specifically, the minke whale (*Balaenoptera acutorostrata*; Murayama et al., 1992), gray whale (*Eschrichtius gibbosus*; Mass & Supin, 1997), Bryde's whale (*Balaenoptera edeni*), and humpback whale (*Megaptera novaeangliae*) (Lisney & Collin, 2018). In these high-resolution zones, the density of retinal ganglion cells provides the retinal resolution expressed in arc minutes of the visual field ranging from 8 arc min in the common dolphin and harbor porpoise to 11.8 arc min in the Pacific white-sided dolphin and beluga.

All the odontocete species listed above are marine dolphins inhabiting relatively clear oceanic waters. A similar organization of the retina with two zones of increased cell densities was also found in a river dolphin, the baiji (*Lipotes vexillifer*), which inhabits low-transparent river and lake waters (Gao & Zhou, 1987). Therefore, this pattern of retinal organization is extensively presented among cetaceans, seemingly irrespective of their phylogenetic position and optic properties of the inhabited environment.

An exception was found in the Amazon river dolphin (*Inia geoffrensis*; Iniidae). This animal has only one retinal zone of higher resolution (Mass & Supin, 1989). Unlike many other cetaceans, the zone of increased cell density in this species is located in a ventral retinal sector and features a low density of ganglion cells that provide a retinal resolution of 40 arc min. This peculiarity of the retina in the Amazon river dolphin was suggested to be associated with inhabiting turbid river water.

The following question arises: "Does the difference between the Amazon river dolphin and the majority of other cetaceans result from the differences in ecology (e.g., water turbidity) or their phylogenetic differences?" An attempt to answer this question was to investigate retinal topography in river dolphins belonging to families which include mostly species with two high-resolution zones in their retinae. Such an investigation was performed in both a representative of the Phocoenidae family, the finless porpoise (*Neophocaena phocaenoides*; Gao & Zhou, 1987), and in a representative of the Delphinidae family, the riverine tucuxi (*Sotalia fluviatilis*; Mass & Supin, 1999). These studies have shown that the retinae in the finless porpoise and tucuxi feature qualitatively the same topographic organization as in marine phocoenids and delphinids—specifically, two zones with a high concentration of ganglion cells. However, retinal resolution resulting from the ganglion cell density in the tucuxi was 25 arc min, which is 2.5 to 3 times less than that in marine delphinids (in the finless porpoise, the cell density of 210 of 250 cells/mm^2 was not converted to retinal resolution). These results may be assessed as a preliminary indication that retinal topography (either two zones of high ganglion cell concentration in the nasal and temporal retinal segments or one zone in the ventral segment) characterizes the phylogenetic position of the species, whereas the high or low density of ganglion cells depends mostly on the optic features of the media.

Results cannot be generalized to all cetaceans, however, because they were obtained in only two species, and information on retinal resolution was available in only one of them. Additionally, whether the specific topographic organization in the Amazon river dolphin (one high-density zone in the ventral part of the retina) and a low concentration of ganglion cells are associated with one another or whether these retinal characteristics are independently influenced by phylogeny and mode of life remain unclear. To obtain more confident conclusions, data on other riverine delphinids are desirable. In this respect, the Irrawaddy dolphin (*Orcaella brevirostris*) may be of interest. This species belonging to the Delphinidae family inhabits lagoons of rivers of Southeast Asia with turbid waters (Stacey & Hvenegaard, 2002; Smith, 2018).

Therefore, the goal of the present study was to investigate the topography of retinal ganglion cells and retinal resolution in the Irrawaddy dolphin. The study was performed using morphological investigation of retinal wholemounts. This method allows us to count all retinal ganglion cells and, thus, to compose a complete map of ganglion cell distribution across the retina and to assess retinal resolution.

Methods

Material

The Irrawaddy dolphin is included in the International Union for Conservation of Nature's (IUCN) *Red List* as "Vulnerable," with several populations assessed as "Extremely endangered" (Smith, 2018). Therefore, the only source of material for morphological investigation could be animals that naturally or accidentally die. In 2007, one dead Irrawaddy dolphin was found tangled in a fishing net in an area of the Mekong River, Vietnam. The body length of this animal was 180 cm. Two eyes of this animal were obtained for investigations.

Eye Enucleation

Both eyes were enucleated. Retinal wholemounts were prepared as described earlier (Mass et al., 2013). Before enucleation, the dorsal pole of the eyeball was marked by a cut. The eyeballs were fixed in 10% buffered formalin; then, the anterior chamber and lens were removed to provide access to the retina. Internal eyecup dimensions and lens sizes were measured.

Retinal Wholemount Preparation

The same procedure was followed for both the left and the right eyes. Briefly, the preparation procedure was as follows: The dorsal pole of the retina was marked by a cut, and the retina was excised from the eyecup. Several radial cuts were made in the retina to allow it to be flattened on a flat glass. The retina was mounted on a glass slide with the ganglion layer facing upward and air dried. Then, the retina was stained by the Nissl method with 0.1% cresyl violet under visual monitoring to stain the ganglion cell layer, not deeper layers. The preparation was dehydrated in alcohols, clarified in xylene, and embedded in Permount (Electron Microscopy Sciences, Hatfield, PA, USA). Since the retina was glued to the glass prior to dehydration, tissue shrinkage was not observed except a slight shrinkage at the edges.

One of the two obtained wholemounts was found to be unsuitable for microscopic investigation because of insufficient tissue preservation, probably because of postmortem degradation. Therefore, only one wholemount was available for analysis.

Microscopic Investigation

For composition of the cell distribution map, the wholemount was inspected with an Olympus BX41 microscope (Shinjuku, Tokyo, Japan) with a low power, a ×20 objective, and a ×10 ocular. The objective was focused on the ganglion cell layer, which was the closest to the surface of the

wholemount. During the inspection, ganglion cells were counted across the entire retinal surface. Counting was performed in samples of 0.5 × 0.5 mm with 0.5 mm steps (1,124 samples; the overall area of 281 mm^2) in zones of high cell concentration or 1 × 1 mm with 1 mm steps (277 samples; the overall area of 277 mm^2) in zones of low cell concentration. Thus, the whole area where the cell densities were counted was 558 mm^2. Cell counts in samples of 0.5 × 0.5 mm were converted to their concentration as the number per 1 mm^2.

For measuring cell sizes, digital photographs were made using a Moticam 2300 digital camera (Motic Hong Kong Limited, Hong Kong) and *Image Plus 2.0* software (Motic Hong Kong Limited).

Data Processing

The cell distribution map was generated based on the cell count data. The map was designed by a custom-made program in the *LabVIEW* program shell (National Instruments [NI], Austin, TX, USA). The program drew isodensity lines by interpolation between samples with cell concentrations immediately above and below the specified density.

To calculate the retinal resolution, we assumed that the mean intercell distance is calculated as follows:

$$d = 1/\sqrt{D},$$

where d is the intercell distance (mm) and D is the cell density (cells/mm^2). This intercell distance in the retina was converted to distance in minutes of visual field as follows:

$$\alpha = 3439d/r,$$

where α is the angular distance, r is the posterior nodal distance, and 3439 serves as the radian/minute ratio. For assessment of the posterior nodal distance, it was assumed that the lens is the only effective refractive structure for underwater vision; therefore, the nodal point is in the center of the lens. The exact position of the lens relative to the retina was not measured because both available eyes were used for wholemount preparation. Based on a previous investigation, we assumed as a first approximation that the lens was concentric with the hemispheric retina. Therefore, the posterior nodal distance was assumed to be equal to the eyecup radius. The obtained angular intercell distance was taken as the retinal resolution in angular minutes.

For cell size assessments, areas of cell profiles were measured in digital photographs. The equivalent cell size was computed as the diameter of a circle of the area equal to that of the cell profile.

Results

Eye Anatomy and Dimensions

The eyeball had a conical shape because the developed retractor muscles were attached to the posterior segment of the eye. The eyecup was flattened in the axial direction and slightly flattened in the dorsoventral direction. The vertical and horizontal outer diameters of the eye from which the analyzed wholemount was obtained were 24 and 26 mm, respectively, with a mean of 25 mm. The eyecup was hemispherical. The internal vertical and horizontal diameters of the eyecup measured after removing the retinae were 21 and 23 mm, respectively, with a mean of 22 mm. Therefore, the radius of the internal eyecup surface was assessed as 11 mm.

The iris had a shape typical of that previously described for many cetaceans—specifically, with a 4-mm protuberance (U-shaped operculum) extending from the dorsal edge of the pupil.

The lens was a slightly flattened sphere. Its transverse diameter was 8 mm, and its axial dimension was 7 mm. As longitudinal sections of the eyes were not prepared, the exact position of the lens relative to the eyecup could not be established. As a first approximation, the position of the lens could be assessed as concentric with the eyecup hemisphere.

A well-developed blue-green tapetum covered almost the entire fundus except for a small dark-pigmented ventral part. The sclera of the eye was thick, the optic nerve output was displaced dorsally relative to the eyecup axis, and the optic nerve diameter was 2.5 mm.

The ganglion cell layer displayed several unstained spots (Figure 1), which might be an indication of retinal postmortem damage. Nevertheless, numerous stained somas of ganglion

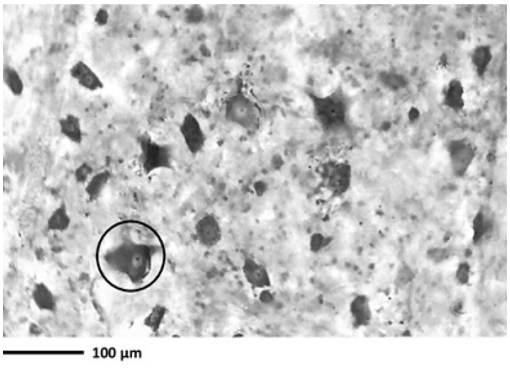

Figure 1. Microphotograph of the ganglion layer. The circle marks a giant ganglion cell. Note the large intercellular distances.

cells were visible. The cells were considered ganglion if they had a polygonal shape, cytoplasm with deeply stained Nissl granules, a nucleus that was lighter than the cytoplasm, and a dark-stained nucleolus inside the nucleus.

The ganglion cell density was rather low. The distances between the nearest cells ranged from 20 to 30 to greater than 100 µm (Figure 1).

Ganglion Cell Topography

The map of ganglion cell distribution displayed rather low cell density (Figure 2). The highest cell density was found in the temporal segment of the retina; this density reached 250 cells/mm^2. Another zone of increased cell density was observed in the nasal segment, where it exceeded 150 cells/mm^2 but did not exceed 200 cells/mm^2. A cell density greater than 250 cells/mm^2 was not observed in any part of the retina.

In more detail, the cell density in- and outside of the high-density zones is illustrated by a plot that presents the cell density distribution along a line that passes through both the high-density zones and the optic disk (Figure 3). This plot shows the cell density maxima of 194 cells/mm^2 in the nasal zone (11.5 mm from the optic disc) and 250 cells/mm^2 in the temporal zone (12 to 12.5 mm from the optic disc).

Giant Cell Topography

Among ganglion cells, a small number had diameters greater than 40 to 50 µm, which substantially exceeded the diameters of the majority of other cells. To ensure that these cells compose a separate group, the ganglion cell size distribution was analyzed. The obtained distribution was bimodal in that it demonstrated the presence of two groups of cells based on differing sizes.

The majority (92%) of cells had sizes ranging from 16 to 36 µm (mean ± SD = 25.4 ± 4.8 µm). A small number (8%) of cells had sizes from 42 to 52 µm (mean ± SD = 45.3 ± 3.8 µm) (Figure 4).

The topographic distribution of these giant cells was mapped separately (Figure 5). Consistent with the low percentage of giant cells, their density never exceeded 9 cells/mm^2. The positions of the highest-density zones for the giant cells were generally the same as those for cells of smaller sizes. Specifically, the highest concentration of 8.6 cells/mm^2 was observed in the temporal segment of the retina; a slightly lower peak density of 7.2 cells/mm^2 was observed in the nasal segment.

To present giant cell density in more detail, their distribution was plotted along a line that passes through both the high-density zones and the optic disk (Figure 6). The plot shows the cell density maxima of 7.2 cells/mm^2 in the nasal zone (7.5 to 8 mm from the optic disk) and 8.6 cells/mm^2 in the temporal zone (14 to 14.5 mm from the optic disk).

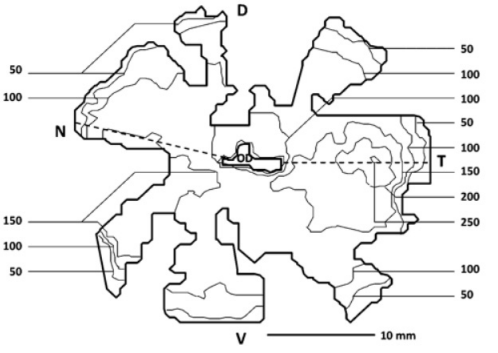

Figure 2. Ganglion cell density map of the wholemount. Isodensity lines delimit zones of cell densities from 50 to 250 cells/mm^2 with steps of 50 cells/mm^2. D, T, V, and N = dorsal, temporal, ventral, and nasal poles, respectively. The dashed line marks the line of cell density plotting for Figure 3.

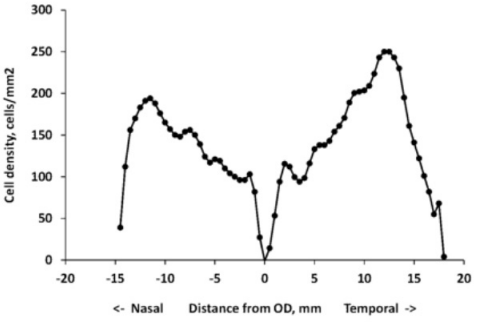

Figure 3. Cell density as a function of distance from the optic disk along the nasal-to-temporal line marked in Figure 2

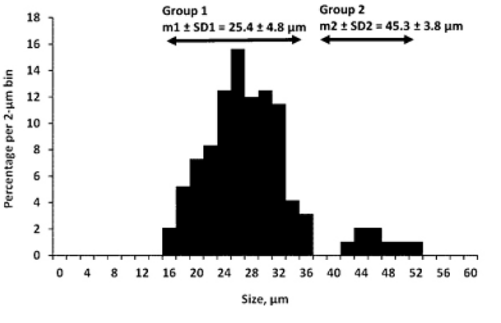

Figure 4. Distribution of ganglion cell diameters: m1 = mean size; SD1 = standard deviation for cells less than 40 µm (Group 1); and m2; SD2 = the same for cells larger than 40 µm (Group 2).

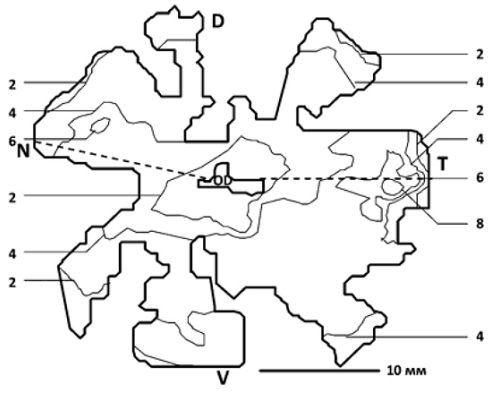

Figure 5. Giant (greater than 40 μm) ganglion cell density map of the wholemount. Isodensity lines delimit zones of cell densities from 2 to 8 cells/mm^2 with steps of 2 cells/mm^2. D, T, V, and N = dorsal, temporal, ventral, and nasal poles, respectively The dashed line marks the line of cell density plotting for Figure 6.

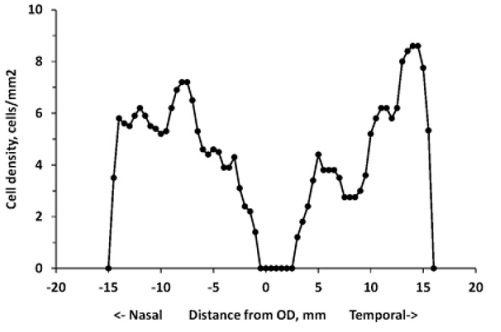

Figure 6. The same as noted in Figure 3 for giant ganglion cells

Retinal Resolution

With a posterior nodal distance of 11 mm and a maximal ganglion cell density in the temporal area of 250 cells/mm^2, the retinal resolution was 19.8 arc min. This retinal resolution is valid for the frontal direction of vision. In the nasal zone (temporal direction of vision), the cell density of 194 cells/mm^2 resulted in a retinal resolution of 22.4 arc min.

Discussion

The weakness of the present study was the limitation of the available material. Specifically, we had only one retinal wholemount that allowed ganglion cell counting. Given these material limitations, we were not capable of statistically assessing how the investigated Irrawaddy dolphin represents the whole population. Nevertheless, we assumed that the available retina was not a unique example that principally differed from those in other individuals. Therefore, we assumed that the obtained data served as a first approach in the assessment of the retinal properties in the Irrawaddy dolphin. These properties can be summarized as follows:

- Anatomical features of the eye were common among many other marine cetaceans previously studied. These features included a conical shape of the eyecup, a hemispheric eyecup slightly flattened in the axial and dorsoventral directions, a typical shape for an iris with an operculum, and a slightly flattened spherical lens. The presence of giant ganglion cells in the retina also resembles that feature in several cetaceans (Dawson et al., 1982; Mass & Supin, 2007; Mass et al., 2013).

- Qualitatively, the pattern of the ganglion-cell layer map was the same as in representatives of several families of marine cetaceans, both odontocetes and mysticetes (see "Introduction"). This pattern is characterized by two zones of ganglion cell concentration—one in the temporal segment and the other in the nasal segment of the retina. Based on this feature, the ganglion cell distribution in the Irrawaddy dolphin is similar to that of a riverine dolphin of the Delphinidae family—namely, the tucuxi (Mass & Supin, 1999); and it differs from that of a riverine dolphin of the Iniidae family—namely, the Amazon river dolphin (Waller, 1982; Mass & Supin, 1989).

- Quantitatively, the cell density in the Irrawaddy dolphin resembles that in riverine dolphins of both the Delphinidae (the riverine tucuxi) and Iniidae (the Amazon river dolphin) families. Respectively, the retinal resolution of 19.8 to 22.4 arc min in the Irrawaddy dolphin is closer to the 25 arc min in the riverine tucuxi (Mass & Supin, 1999) and the 8 to 10 arc min in marine odontocetes (Herman et al., 1975; Dral, 1983; Mass & Supin, 1995; Murayama et al., 1995; Mass et al., 2013), although higher than the 40 arc min in the Amazon river dolphin (Mass & Supin, 1989).

Thus, by combining the data obtained in riverine dolphins both in previous investigations in the finless porpoise and baiji (Gao & Zhou, 1987), the Amazon river dolphin (Mass & Supin, 1989), and the tucuxi (Mass & Supin, 1999) and in the Irrawaddy dolphin in the present study, we can suggest the following:

- The specific pattern of ganglion cell distribution that is characterized by the presence of two areas of ganglion cell concentration is characteristic of many, but not all, delphinid families, independent of whether they inhabit clear oceanic waters or turbid river waters. The pattern that is characterized by one spot of ganglion cell concentration in the ventral part of the retina is characteristic of the Iniidae family (not considering families that have not been investigated to date).

- The low density of ganglion cells is associated with optic properties of the media and is characteristic of dolphin species inhabiting turbid river waters, including members of both Delphinidae and Iniidae (again, not considering families that were not investigated to date).

Acknowledgments

The study was performed using equipment from the Instrumental Methods in Ecology Center of the Institute of Ecology and Evolution. Authors thank M. B. Tarakanov for his help in collecting the material. The valuable assistance of R. M. Khatsaeva, A. Podzolkova, and A. Neretina in processing the microphotographs is greatly appreciated.

Literature Cited

Coimbra, J. P., & Manger, P. R. (2017). Retinal ganglion cell topography and spatial resolving power in the white rhinoceros (*Cedratotherium simum*). *Journal of Comparative Neurology*, *525*(11), 2484-2498. https://doi.org/10.1002/cne.24136

Coimbra, J. P., Bertelsen, M. F., & Manger, P. R. (2017). Retinal ganglion cell topography and spatial resolving power in the river hippopotamus *Hippopotamus amphibious*. *Journal of Comparative Neurology*, *525*(11), 2499-2513. https://doi.org/10.1002/cne.24179

Collin, S. P. (1999). Behavioural ecology and retinal cell topography. In S. N. Archer, M. B. A. Djamgoz, E. R. Loew, J. V. C. Partridge, & S. Vallerga (Eds.), *Adaptive mechanisms in the ecology of vision* (pp. 509-535). Springer. https://doi.org/10.1007/978-94-017-0619-3_17

Dawson, W. W., Hawthorne, M. N., Jenkins, R. L., & Goldston, R. T. (1982). Giant neural system in the inner retina and optic nerve of small whales. *Journal of Comparative Neurology*, *205*(1), 1-7. https://doi.org/10.1002/cne.902050102

Dral, A. D. G. (1983). The retinal ganglion cells of *Delphinus delphis* and their distribution. *Aquatic Mammals*, *10*(2), 57-68.

Gao, A., & Zhou, K. (1987). On the retinal ganglion cells of *Neophocaena* and *Lipotes*. *Acta Zoologica Sinica*, *33*(4), 316-332.

Herman, L. M., Peacock, M. F., Yunker, M. P., & Madsen, C. J. (1975). Bottle-nosed dolphin: Double-slit pupil yields equivalent aerial and underwater diurnal acuity. *Science*, *189*(4203), 650-652. https://doi.org/10.1126/science.1162351

Hughes, A. (1977). The topography of vision in mammals of contrasting life style: Comparative optics and retinal organisation. In F. Crescitelli (Ed.), *Handbook of sensory physiology: Vol. VII. The visual system of vertebrates* (pp. 613-756). Springer. https://doi.org/10.1007/978-3-642-66468-7_11

Lisney, T. J., & Collin, S. P. (2018). Retinal topography in two species of baleen whale (Cetacea: Mysticeti). *Brain, Behavior and Evolution*, *92*(3-4), 97-116. https://doi.org/10.1159/000495285

Mass, A. M., & Supin, A. Ya. (1986). Topographic distribution of size and density of ganglion cells in the retina of a porpoise, *Phocoena phocoena*. *Aquatic Mammals*, *12*(3), 95-102.

Mass, A. M., & Supin, A. Ya. (1989). Distribution of ganglion cells in the retina of an Amazon river dolphin *Inia geoffrensis*. *Aquatic Mammals*, *15*(2), 49-56.

Mass, A. M., & Supin, A. Ya. (1995). Retinal cell topography of the retina in the bottlenose dolphin *Tursiops truncatus*. *Brain, Behavior and Evolution*, *45*(5), 257-265. https://doi.org/10.1159/000113554

Mass, A. M., & Supin, A. Ya. (1997). Ocular anatomy, retinal ganglion cell distribution, and visual resolution in the gray whale, *Eschrichtius gibbosus*. *Aquatic Mammals*, *23*(1), 17-28.

Mass, A. M., & Supin, A. Ya. (1999). Retinal topography and visual acuity in the riverine tucuxi (*Sotalia fluviatilis*). *Marine Mammal Science*, *1*(2), 351-365. https://doi.org/10.1111/j.1748-7692.1999.tb00806.x

Mass, A. M., & Supin, A. Ya. (2002). Visual field organization and retinal resolution of the beluga, *Delphinapterus leucas* (Pallas). *Aquatic Mammals*, *28*(3), 241-250.

Mass, A. M., & Supin, A. Ya. (2007). Adaptive features of aquatic mammal's eye. *Anatomical Record*, *290*(6), 701-715. https://doi.org/10.1002/ar.20529

Mass, A. M., Supin, A. Ya., Abramov, A. V., Mukhametov, L. M., & Rozanova, E. I. (2013). Ocular anatomy, ganglion cell distribution, and retinal resolution of a killer whale (*Orcinus orca*). *Brain, Behavior and Evolution*, *81*(1), 1-11. https://doi.org/10.1159/000341949

Murayama, T., & Somiya, H. (1998). Distribution of ganglion cells and object localization ability in the retina of three cetaceans. *Fisheries Science*, *64*(1), 27-30. https://doi.org/10.2331/fishsci.64.27

Murayama, T., Somiya, H., Aoki, I., & Ishii, T. (1992). The distribution of ganglion cells in the retina and visual acuity of minke whale. *Nipping Susan Gikkaishi*, *58*(6), 1057-1061. https://doi.org/10.2331/suisan.58.1057

Murayama, T., Somiya, H., Aoki, I., & Ishii, T. (1995). Retinal ganglion cell size and distribution predict visual capabilities of Dall's porpoise. *Marine Mammal Science*, *11*(2), 136-149. https://doi.org/10.1111/j.1748-7692.1995.tb00513.x

Pettigrew, J. D., & Manger, P. R. (2008). Retinal ganglion cell density of the black rhinoceros (*Diceros bicornis*):

Calculating visual resolution. *Visual Neuroscience*, *25*(2), 215-220. https://doi.org/10.1017/S0952523808080498

Pettigrew, J. D., Bhagwandin, A., Haagensen, N., & Manger, P. R. (2010). Visual acuity and heterogeneities of retinal ganglion cell densities and the tapetum lucidum of the African elephant (*Loxodonta africana*). *Brain, Behavior and Evolution*, *75*(4), 251-261. https://doi.org/10.1159/000314898

Smith, B. D. (2018). Irrawaddy dolphin. In B. Würsig, J. G. M. Thewissen, & K. M. Kovacs (Eds.), *Encyclopedia of marine mammals* (pp. 525-529). Academic Press. https://doi.org/10.1016/B978-0-12-804327-1.00161-8

Stacey, P. J., & Hvenegaard, G. T. (2002). Habitat use and behaviour of Irrawaddy dolphins (*Orcaella brevirostris*) in the Mekong River of Laos. *Aquatic Mammals*, *28*(1), 1-13.

Waller, G. N. H. (1982). Retinal ultrastructure of the Amazon river dolphin (*Inia geoffrensis*). *Aquatic Mammals*, *9*(1), 17-28.